Available online at www.sciencedirect.com

ScienceDirect

Trans. Nonferrous Met. Soc. China 23(2013) 2002−2010

Transactions of
Nonferrous Metals
Society of China

www.tnmsc.cn

# Tribological behavior and mechanism of NiCrBSi−$Y_2O_3$ composite coatings

Bin CAI, Ye-fa TAN, Hua TAN, Qi-feng JING, Zhong-wei ZHANG

College of Field Engineering, PLA University of Science and Technology, Nanjing 210007, China

Received 5 June 2012; accepted 5 December 2012

**Abstract:** The NiCrBSi−$Y_2O_3$ composite coatings were prepared on the surface of 45 carbon steel by plasma spray, the microstructure and tribological properties of the coatings were investigated. The results show that the NiCrBSi−$Y_2O_3$ composite coatings are mainly composed of $\gamma$-Ni, CrB, $Cr_7C_3$ and $Y_2O_3$. With addition of $Y_2O_3$, hard phases such as CrB, $Cr_7C_3$ emerge in composite coating, and the density of the composite coatings also increases. The NiCrBSi−0.5$Y_2O_3$ composite coating presents excellent tribological properties. Its friction coefficient is 0.175, which is about 37% of that of the pure NiCrBSi coating. The mass wear loss is 1.2 mg, which is reduced by 43% compared with the pure NiCrBSi coating. When the loads are 6−10 N, the NiCrBSi−0.5$Y_2O_3$ composite coating suffers from slight wear and the wear mechanisms are mainly adhesive wear accompany with slight micro-cutting wear and micro-fracture wear. As the load increases to 12 N, the wear mechanisms are adhesive wear and severe micro-cutting wear.

**Key words:** plasma spray; composite coating; NiCrBSi; $Y_2O_3$; friction; wear

## 1 Introduction

The parts used in metallurgical and construction machinery usually suffer from severe friction and wear, the anti-wear alloy coatings are widely applied to improving their wear resistance and prolong their sevice lives [1,2]. However, the values of friciton coefficients of the anti-wear alloy coatings are usually high, thus leading to high energy consumption [3,4]. As the mechanical equipments develop, the mechine parts are getting more demands on anti-friciton property. So, it becomes research hotspot to develope the surface coatings with both property of anti-wear and low friction coefficients.

Rare earth oxides such as $CeO_2$ and $La_2O_3$ are commonly used to improve mechanical property and wear resistance of surface coatings. For example, the microhardness and wear resistance of the laser clad $TiC_p$/Ni-base alloy composite coatings could be improved by adding 0.5% $La_2O_3$ (in mass fraction), and friction coefficient of the composite coatings was also reduced [5]. With addition of 1.5% $Sm_2O_3$ (in mass fraction), the microstructure of the laser cladded Ni-based alloy coating could be refined and the microhardness increased from $HV_{0.2}$ 484 to $HV_{0.2}$ 712. The wear rate of the composite coatings was reduced by 50% compared with the pure Ni-based alloy coatings [6]. WANG et al [7] found that the microhardness of the spray welded Ni-based alloy coating decreased with addition of 4%$La_2O_3$ (in mass fraction), and its mass wear loss was reduced by 20% compared with the coating without $La_2O_3$. That is because $La_2O_3$ can improve the uniformity of the coating microstructure and its resistance to micro-cutting. It can be concluded that rare earths not only improve wear resistance but also have the effects of anti-friction.

Wear resistance of surface coatings with rare earths increases because the microstructure of surface coatings is refined and purified, so their hardness and fracture toughness increase [8−10]. However, there are different views on the anti-friction mechanisms of rare earths in surface coatings. For example, ZHANG et al [11] considered that rare earth oxides have the character as solid lubricant. HAN and LU [12] attributed the anti-friction effects of $CeO_2$ not only to its hexagonal structure, but also to the reduction of micro-cutting force for the improved density of the composite coatings. HUANG et al [13] reckoned that rare earth refined the coating structure and improved the fracture toughness of the coating, so reduced the friction coefficients.

Researches on anti-wear and anti-friction effects of

---

**Corresponding author:** Ye-fa TAN; Tel: +86-25-80821055; E-mail: tanyefa7651@163.com

DOI: 10.1016/S1003-6326(13)62689-8

rare earths are mainly focused on coatings prepared by fused cladding technology such as laser cladding and induction cladding, but the mechanisms of rare earths in the plasma spray technology are different from those in the fused cladding technology, which need to be researched. The temperature of the substrate is low in plasma spray process and the solidification speed of the sprayed particles is higher than $10^5$ °C/s [14]. In addition, the $Y_2O_3$ particles may act as the better heterogeneous nucleation than $La_2O_3$ and $CeO_2$ particles, which may improve the uniformity of the hard phase and the microhardness of the coatings [15]. In this work, the NiCrBSi−$Y_2O_3$ composite coatings were prepared on the surface of 45 carbon steel by plasma spray technology, the microstructure, microhardness and tribological properties of the composite coatings were investigated to provide theory basis and experimental data for application of $Y_2O_3$ in the plasma spray coatings.

## 2 Experimental

### 2.1 Specimen preparation

The NiCrBSi−$Y_2O_3$ composite materials are composed of NiCrBSi powders and $Y_2O_3$ powders. The chemical composition of the NiCrBSi powders was 16Cr, 3.1B, 4.3Si, 4Fe, 0.65C and balance Ni (mass fraction, %) and its particle sizes were in the range of 55−128 μm. The purity of $Y_2O_3$ powders with sizes of 15−45 μm was 99.5%. The composite spray powders were made by the mixture of the Ni-based alloy powders and the $Y_2O_3$ powders in a ball mill equipment for 1 h.

The 45 carbon steel was chosen as the substrate, and was previously treated by surface degrease and sand spraying. The composite powders were respectively sprayed on the surface of 45 carbon steel by the plasma spray equipment of DH1080. The spray technological parameters were electric current of 600 A, voltage of 40 V and spray distance of 80 mm. The thickness of the spray coating was 400 μm with surface roughness of 0.5 μm after being ground by diamond wheel.

### 2.2 Tribological tests

The tribological tests were carried out in a ball-on-disc tribometer of HT-500. The upper specimen was GCr15 steel ball with the diameter of 4 mm and the surface roughness of 0.05 μm. The down ones were the composite coatings. Tribological tests were conducted at the speed of 0.1 m/s in room temperature, normal load was 6−12 N, and sliding distance was 360 m. The mass wear losses of the specimens were measured by the balance of TG328A with accuracy of 0.1 mg.

### 2.3 Surface analysis

The X-ray diffraction (XRD) of the composite coatings was performed on a D/max 2500 X-ray diffractometer. Porosity of the coatings was tested by the DM−3000 metallography analysis software. The microhardness of the coatings was measured using the DHV−1000 sclerometer under the load of 4.92 N with a dwell time of 15 s. The morphologies of the microstructure and the worn surface of the composite coatings were observed by the scanning electron microscope (SEM) of QUANTA 200. Chemical composition of the composite coatings was analyzed with the energy-dispersive analysis of X-ray (EDAX).

## 3 Results and discussion

### 3.1 Microstructure of NiCrBSi−$Y_2O_3$ composite coatings

The XRD patterns of the NiCrBSi−$Y_2O_3$ composite coatings are shown in Fig. 1. It can be found that the NiCrBSi−$Y_2O_3$ composite coatings are mainly composed of $\gamma$-Ni, CrB, $Cr_7C_3$ and $Y_2O_3$. Compared with the pure NiCrBSi coating, there are some new phases such as CrB and $Cr_7C_3$ emerge in the NiCrBSi−0.5$Y_2O_3$ composite coating. During the spraying process, the NiCrBSi powders and the $Y_2O_3$ powders were heated and fused by the plasma flame, and then the fused particles quickly solidified on the substrate of the carbon steel. It was reported that element C can promote the decomposition of rare earth oxides into rare earth elements during solidification process of the fused particles [16], so $Y_2O_3$ may react with C to produce Y:

$$Y_2O_3+3[C]=2[Y]+3CO \tag{1}$$

The solid solubility of Y in NiCrBSi is low because the large radius of Y is 0.18 nm [17]. This may account for the segregation of Y at the dislocation and grain boundary area of the NiCrBSi coating, which leads

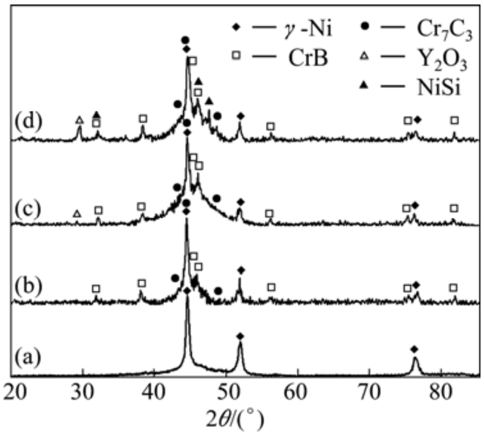

**Fig. 1** XRD patterns of NiCrBSi−$Y_2O_3$ composite coatings: (a) Pure NiCrBSi coating; (b) NiCrBSi−0.5$Y_2O_3$ composite coating; (c) NiCrBSi−1.0$Y_2O_3$ composite coating; (d) NiCrBSi−2.0$Y_2O_3$ composite coating

to distortion area in the coating [18]. Y has a strong adsorptive action to elements C and B [19], so it causes segregation of elements C and B in the distortion area. As the concentrations of elements C and B increase to certain degree at the distortion area, CrB and $Cr_7C_3$ may precipitate. So, the diffraction peaks of CrB and $Cr_7C_3$ emerge in the NiCrBSi−0.5$Y_2O_3$ composite coating, which indicates that $Y_2O_3$ may promote the precipitation of CrB and $Cr_7C_3$ in the composite coatings. The hard phases of CrB and $Cr_7C_3$ can improve the wear resistance of the composite coatings.

As $Y_2O_3$ increases to 1.0% (in mass fraction), CrB in the composite coating increases compared with the NiCrBSi−0.5$Y_2O_3$ composite coating. It also shows a little $Y_2O_3$ in the composite coating which indicates some unreacted $Y_2O_3$ particles retained in the composite coating. The CrB content is improved due to the heterogeneous nucleation effects of the unreacted $Y_2O_3$ particles.

When $Y_2O_3$ is 2.0%, the new phase of NiSi emerges in the composite coating. The unreacted $Y_2O_3$ particles retained in the composite coating increase as $Y_2O_3$ content increases, which enhances the heterogeneous nucleation effect and promotes the precipitation of brittle composites, such as NiSi. Therefore, the brittleness of the composite coating increases. It can be concluded that the optimum addition of 0.5% $Y_2O_3$ may improve the hard phases of CrB and $Cr_7C_3$ in the composite coating, but excess $Y_2O_3$ may induce brittle phases such as NiSi in the composite coatings and result in higher brittleness.

Figure 2 shows the metallographic pictures of the pure NiCrBSi coating and the NiCrBSi−0.5$Y_2O_3$ composite coating. The grain size of the latter is smaller than that of the former. This indicates that $Y_2O_3$ may refine the grain size of the NiCrBSi coating.

Figure 3 shows the porosity of the NiCrBSi−$Y_2O_3$ composite coatings as a function of $Y_2O_3$ content. The porosity initially decreases and then increases with increasing $Y_2O_3$ content. It is observed that the porosity of the composite coatings is much lower than that of the pure NiCrBSi coating (porosity of 2.96%). It is 0.92% when the $Y_2O_3$ content is 0.5%, and then reaches the lowest value (about 0.67%) as the $Y_2O_3$ content increases to 1.0−1.5%. It is well known that porosity of the sprayed coatings is closely related to the deformation degree of the fused particles. It was reported that the deformation degree of the fused particles during plasma spray can be demonstrated as Eq. (2) [20]:

$$\frac{D}{h}=\frac{\rho d v^2}{2\sigma}+3 \tag{2}$$

where $\sigma$ is the surface tension of the fused particles; $\rho$ is density of the particles; $d$ is the size of the particles; $D/h$ is the ratio of size to height of the particles on the substrate. The higher the value of $D/h$ is, the more flat the particles become.

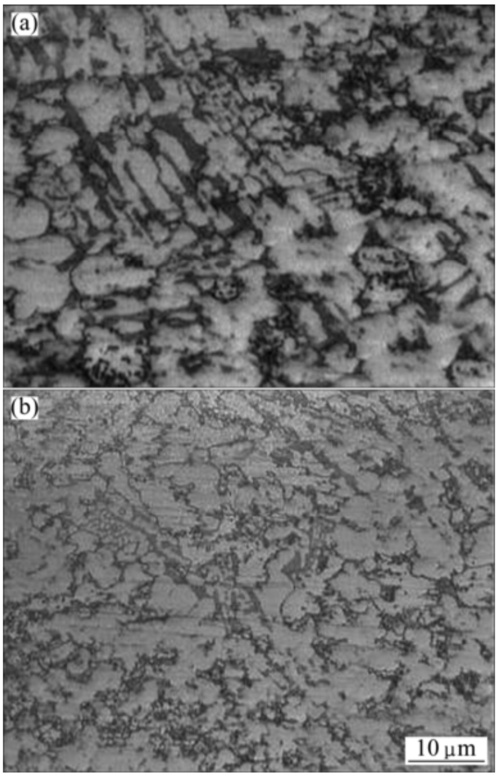

**Fig. 2** Metallographic pictures of pure NiCrBSi coating (a) and NiCrBSi−0.5$Y_2O_3$ composite coating (b)

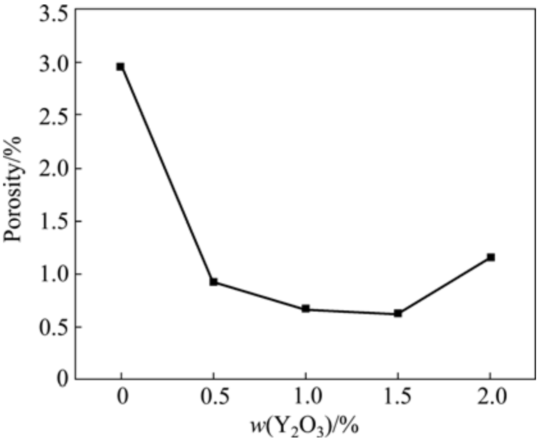

**Fig. 3** Porosity of NiCrBSi−$Y_2O_3$ composite coatings

Rare earths can improve the wettability of the NiCrBSi particles due to their high activity [21], so $\sigma$ of the NiCrBSi powders decreases with addition of $Y_2O_3$, which means the value of $D/h$ increases. Figure 4 shows the sprayed particles morphology of the pure NiCrBSi powders and the NiCrBSi−0.5$Y_2O_3$ composite powders. The spread particles in the composite powders with $Y_2O_3$ (as shown in Fig. 4(b)) are larger than those in the pure NiCrBSi powders (as shown in Fig. 4(a)), which indicates the fused particles of the NiCrBSi−$Y_2O_3$

composite coatings are more flat and compact than those of the coatings without $Y_2O_3$. This may account for the decreasing porosity of the NiCrBSi−$Y_2O_3$ composite coatings.

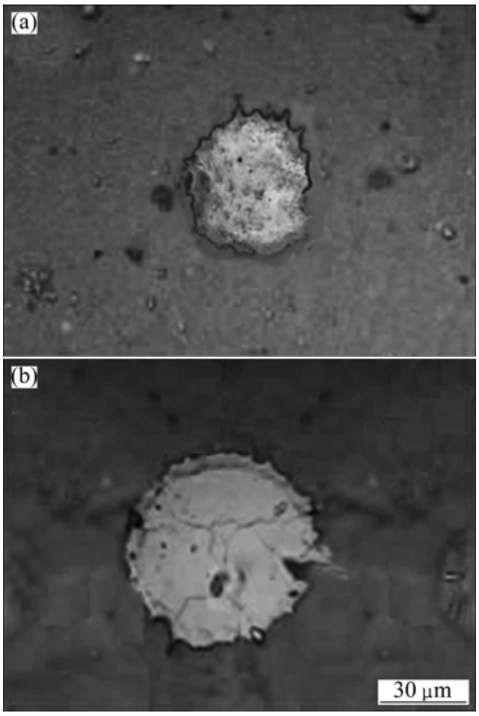

**Fig. 4** OM images showing sprayed particles morphology of pure NiCrBSi powder (a) and NiCrBSi−0.5$Y_2O_3$ composite powders (b)

However, the porosity of the composite coatings increases to 1.16% when the $Y_2O_3$ content is 2.0% because the unreacted $Y_2O_3$ particles may induce defects such as voids and pores in the composite coating.

Microhardness of the NiCrBSi−$Y_2O_3$ composite coatings as a function of $Y_2O_3$ content is shown in Fig. 5. The average microhardness of the NiCrBSi−$Y_2O_3$ composite coatings is HV 700, which is found to dramatically increase compared with the pure NiCrBSi coating (HV 586). It can be attributed to the following reasons: 1) Plastic deformation of the composite coatings after microhardness test decreases because of the increased density due to the decrease of porosity with addition of $Y_2O_3$; 2) The hard phase precipitates such as CrB and $Cr_7C_3$ are improved by $Y_2O_3$, which can increase the microhardness of the composite coatings.

## 3.2 Effects of $Y_2O_3$ content on tribological behavior and mechanisms of composite coatings

The friction coefficients of the NiCrBSi−$Y_2O_3$ composite coatings with the increasing $Y_2O_3$ content are shown in Fig. 6. The friction coefficients initially decrease and then increase and lastly remain unchanged.

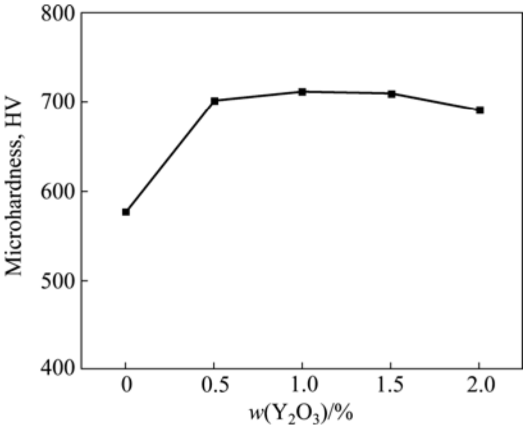

**Fig. 5** Microhardness of NiCrBSi−$Y_2O_3$ composite coatings

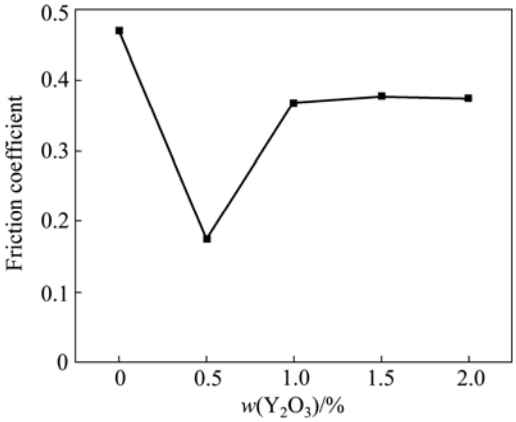

**Fig. 6** Friction coefficients of NiCrBSi−$Y_2O_3$ composite coatings (load=10 N)

The friction coefficient of NiCrBSi−0.5$Y_2O_3$ composite coating (0.175) is much lower than that of the pure NiCrBSi coating (0.47). As the $Y_2O_3$ content increases to 1.0%, the friction coefficient is 0.36, which is higher than that of the NiCrBSi−0.5$Y_2O_3$ composite coating. The friction coefficient remains at 0.37 when $Y_2O_3$ is 2.0%.

Figure 7 shows the wear mass loss of the NiCrBSi−$Y_2O_3$ composite coatings as a function of $Y_2O_3$ content. The wear mass losses of the composite coatings firstly decrease and then increase. The wear mass loss of the NiCrBSi−0.5$Y_2O_3$ composite coating is 1.2 mg, reduced by 43% compared with the pure NiCrBSi coating (2.1 mg). That is because the microhardness of the former is higher than the latter. The mass loss wear of the NiCrBSi−1.0$Y_2O_3$ composite coating is the lowest (0.9 mg). When $Y_2O_3$ exceeds 1.0%, the wear mass losses of the composite coatings increase. For example, the wear mass loss of the NiCrBSi−2.0$Y_2O_3$ is 1.6 mg.

Figure 8 shows the worn surface of the pure NiCrBSi coating with its EDAX spectrum. Some worn furrows emerge on the worn surface, as shown in Fig. 8(a), because the solid welding nodes in the contact

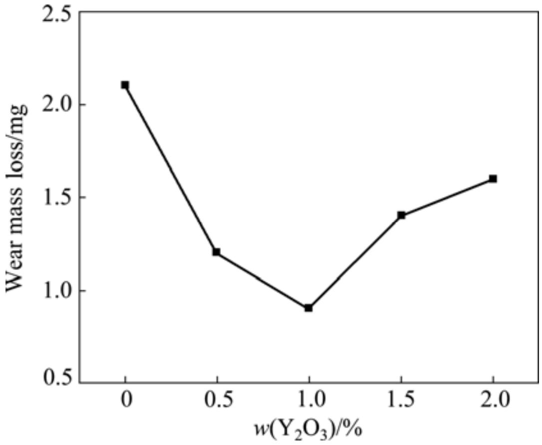

**Fig. 7** Wear mass loss of NiCrBSi−$Y_2O_3$ composite coatings under load of 10 N

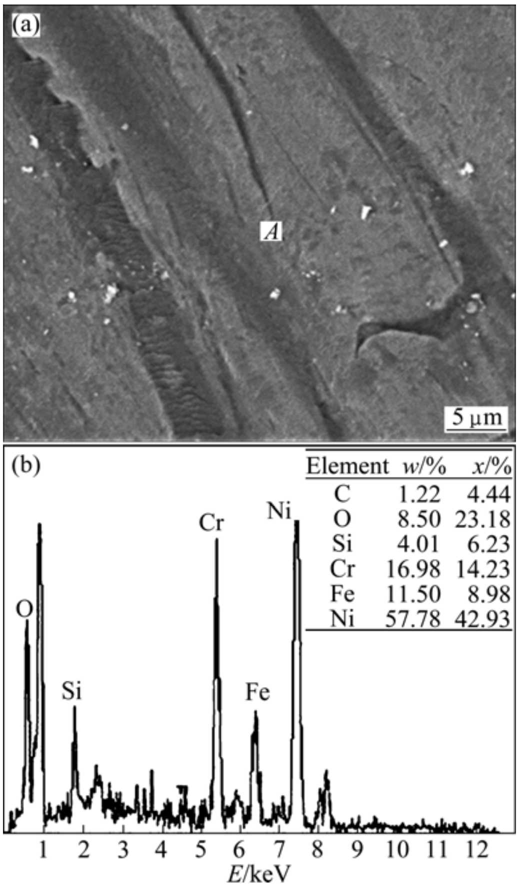

| Element | w/% | x/% |
|---|---|---|
| C | 1.22 | 4.44 |
| O | 8.50 | 23.18 |
| Si | 4.01 | 6.23 |
| Cr | 16.98 | 14.23 |
| Fe | 11.50 | 8.98 |
| Ni | 57.78 | 42.93 |

**Fig. 8** SEM image showing worn surface morphology (a) and EDAX spectrum (b) of pure NiCrBSi coating

area between the pure NiCrBSi coating and GCr15 steel ball suffer from shear damage and lead to plastic flow of the surface materials. The chemical composition of the worn surface is 1.22C, 8.50O, 4.01Si, 16.98Cr, 11.50Fe and 57.78Ni (mass fraction, %) according to Fig. 8(b). The content of element Fe is 11.50% on the worn surface, which is about 2.9 times that in the NiCrBSi powders because the GCr15 steel ball materials transfer to the worn surface of the pure NiCrBSi coating as a result of shear damage of the solid welding nodes. The friction coefficient of the pure NiCrBSi coating is relatively high because of severe adhesive friction. In addition, the grooves on the worn surface indicate micro-cutting wear of the composite coating, so the main wear mechanisms of the pure NiCrBSi coating are adhesive wear and micro-cutting wear.

The friction coefficients and wear mass loss of the NiCrBSi−0.5$Y_2O_3$ composite coating are greatly reduced compared with the pure NiCrBSi coating. Figure 9 shows the worn surface of the NiCrBSi−0.5$Y_2O_3$ composite coating and its EDAX spectrums. Figure 9(a) shows that a dark grey film emerges on the worn surface. The chemical composition of the film is 2.42C, 9.88O, 3.18Si, 15.99Cr, 7.36Fe and 61.18Ni (mass fraction, %) (Fig. 9(b)), which indicates $Fe_2O_3$, $Fe_3O_4$ and NiO in the film. The film may easily shear under the friction force and lead to greatly decrease of the shear strength at the friction interface. So, the friction coefficients of the NiCrBSi−0.5$Y_2O_3$ composite coating decrease. The vacancy density increases in the friction surface because of the increased temperature induced by friction heat. Then Y at the grain boundary is more apt to diffuse and segregate in the vacancies than other alloying elements for its low free energy. The segregated rare earth on the

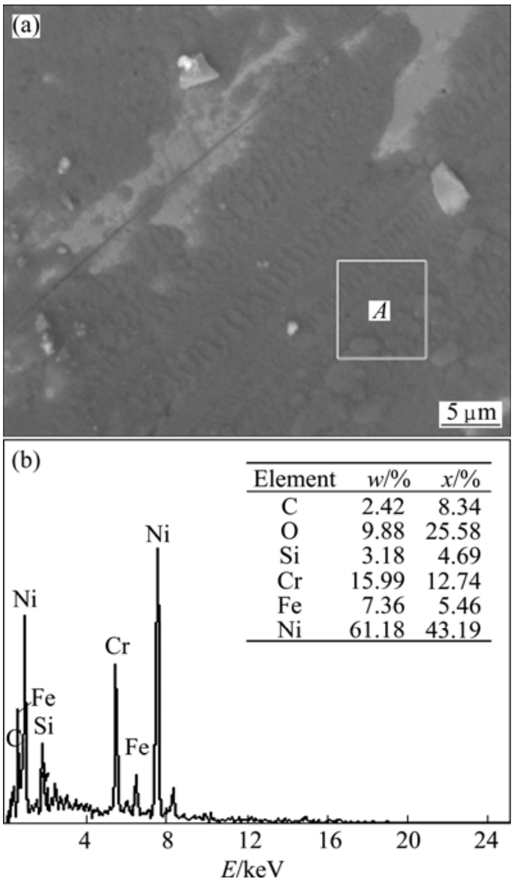

| Element | w/% | x/% |
|---|---|---|
| C | 2.42 | 8.34 |
| O | 9.88 | 25.58 |
| Si | 3.18 | 4.69 |
| Cr | 15.99 | 12.74 |
| Fe | 7.36 | 5.46 |
| Ni | 61.18 | 43.19 |

**Fig. 9** SEM image showing worn surface morphology (a) and EDAX spectrum (b) of NiCrBSi−0.5$Y_2O_3$ composite coating

friction surface can reduce vacancies and voids between the oxide film and the substrate, which results in the increasing combined strength of the oxide film. As a result, the complete oxide film is developed on the worn surface.

The content of element Fe on the worn surface is 7.46%, much less than that in the worn surface of the pure NiCrBSi coating. This suggests that the adhesive action is alleviated because of less GCr15 steel transferred to the worn surface. It can be concluded that the oxide film on the worn surface of the NiCrBSi−0.5$Y_2O_3$ composite coating can not only reduce friction coefficients, but also reduce adhesive wear. Besides, the lump wear debris are found on the worn surface of the composite coating as shown in Fig. 9(a), which indicates certain extent brittle fracture of the coating. It shows that the wear mechanisms of the NiCrBSi−0.5$Y_2O_3$ composite coating are mainly slight adhesive wear accompany with slight micro-fracture wear.

The wear behavior and mechanisms of the NiCrBSi−$Y_2O_3$ composite coatings change with the further increase of $Y_2O_3$ content. The worn surface of the NiCrBSi−1.0$Y_2O_3$ composite coating and its EDAX spectrum are shown in Fig. 10. It is obvious that many black point-like structures distribute on the smooth worn surface with little oxide film as shown in Fig. 10(a). The chemical composition of the point-like structures is 1.15% C, 9.64% O, 0.76% Si, 82.16% Cr, 1.63% Fe, 3.59% Ni and 1.08% Y (Fig. 10(b)). It shows that the point-like structures are rich in Cr, indicating that the point-like structures are mainly CrB and $Cr_7C_3$. These hard phases are exposed on the worn surface and support the GCr15 steel ball after the alloy matrix around the hard phases wears off during friction process. Thus the hard phases bear main load and induce great decrease in pressure on the Ni-based alloy matrix, which results in reduction of the friction heat by plastic deformation. Therefore, friction oxidation reaction of the Ni-based alloy matrix is too little to produce oxide film which can account for the increase in friction coefficient of the NiCrBSi−1.0$Y_2O_3$ composite coating.

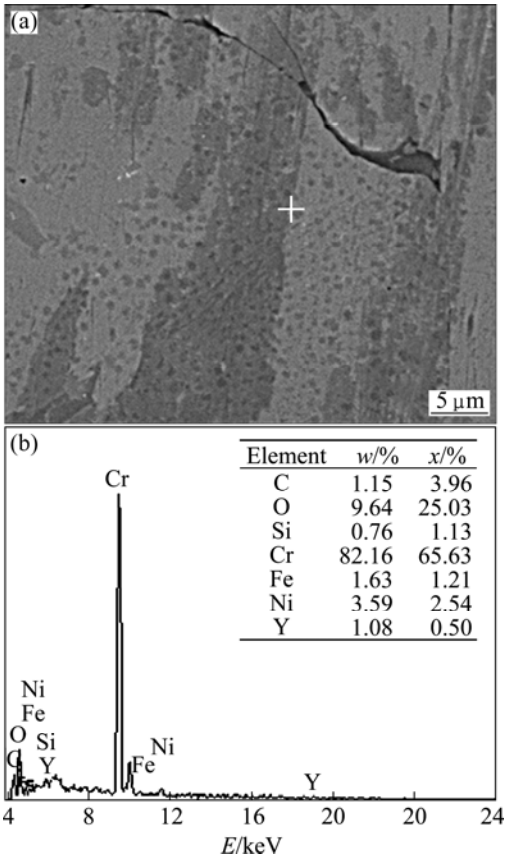

| Element | w/% | x/% |
|---|---|---|
| C | 1.15 | 3.96 |
| O | 9.64 | 25.03 |
| Si | 0.76 | 1.13 |
| Cr | 82.16 | 65.63 |
| Fe | 1.63 | 1.21 |
| Ni | 3.59 | 2.54 |
| Y | 1.08 | 0.50 |

**Fig. 10** SEM image showing worn surface morphology (a) and EDAX spectrum (b) of NiCrBSi−1.0$Y_2O_3$ composite coating

The wear mass loss of the NiCrBSi−1.0$Y_2O_3$ composite coating is lower than that of the NiCrBSi−0.5$Y_2O_3$ composite coating, because the former coating is more resistant to plastic deformation than the latter due to its higher microhardness than the latter. Some micro-cracks and fracture pits emerge on the worn surface of the composite coating (Fig. 10(a)). These micro-cracks can be attributed to the stress concentration in the combine region between the hard phases and the Ni-based alloy matrix as a result of high shear force on the hard phases during friction. This suggests that the main wear mechanisms of the NiCrBSi−1.0$Y_2O_3$ composite coating are mainly adhesive wear and micro-fracture wear.

Figure 11 shows the worn surface of the NiCrBSi−1.5$Y_2O_3$ composite coating and there are more micro-cracks on its worn surface than on the NiCrBSi−1.0$Y_2O_3$ composite coating, and some micro-cutting grooves are produced on the worn surface. Due to the increasing brittleness phases in the NiCrBSi−1.5$Y_2O_3$ composite coating, there are the micro-cracks and micro-fracture in the composite coating caused by the shear force increase. The micro-cutting grooves are plough by wear debris on the worn surface and lead to increase of wear mass loss. Main wear mechanisms of the NiCrBSi−1.5$Y_2O_3$ composite coating are micro-fracture wear and micro-cutting wear.

As the $Y_2O_3$ content increases to 2.0%, many micro-cracks and micro-cutting grooves emerge on the worn surface of the composite coating (Fig. 12). The increased porosity of the composite coating causes more defects in the coating. These defects develop to micro-cracks under cyclic load, and lead to fracture of the worn surface materials which act as wear debris. The wear debris induces three-body abrasive wear, so the micro-cutting grooves increase in Fig. 12. As a result, micro-fracture wear and micro-cutting wear of the NiCrBSi−2.0$Y_2O_3$ composite coating increase compared with the NiCrBSi−1.5$Y_2O_3$ composite coating.

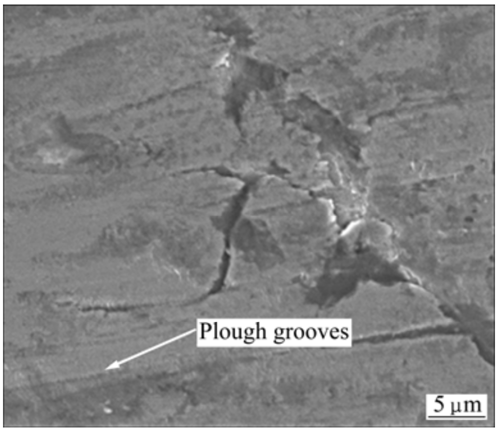

**Fig. 11** SEM image showing worn surface morphology of NiCrBSi−1.5$Y_2O_3$ composite coating

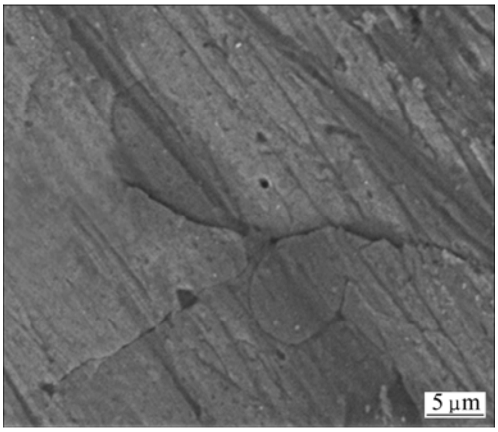

**Fig. 12** SEM image showing worn surface morphology of NiCrBSi−2.0$Y_2O_3$ composite coating

It can be concluded that the NiCrBSi−0.5$Y_2O_3$ composite coating presents excellent tribological properties, whose friction coefficient is 0.175 which is 37% of that of the pure NiCrBSi coating. The wear mass loss of the composite coating is 1.2 mg, which is reduced by 43% compared with the pure NiCrBSi coating. The decreased friction coefficient of the composite coating can be attributed to the solid lubrication effect of the oxide film on the worn surface.

### 3.3 Effects of load on tribological properties of NiCrBSi−$Y_2O_3$ composite coatings

The effects of load on tribological properties of the NiCrBSi−0.5$Y_2O_3$ composite coating are researched in consideration of its excellent tribological properties. Figure 13 shows the friction coefficients and wear mass losses of the NiCrBSi−0.5$Y_2O_3$ composite coating as a function of load. Its friction coefficients take on a slight decrease trend as the load increases, which is in the range of 0.173 and 0.18. The wear mass losses of the composite coating increase with the increasing load. Under at the loads of 6−10 N, the composite coating suffers from slight wear and the wear mass losses are between 0.7 mg and 1.2 mg. As the load exceeds 10 N, the mass wear loss increases to 2.7 mg, indicating severe wear of the composite coating.

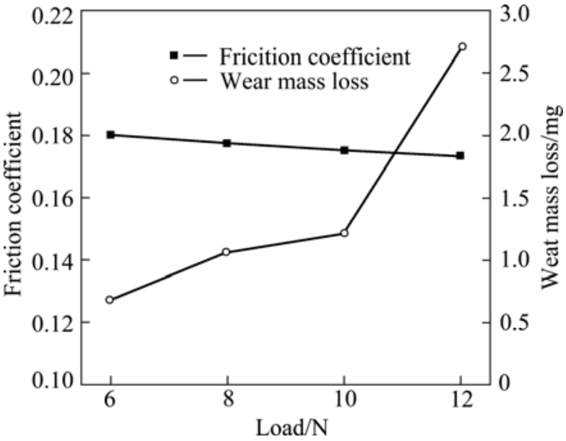

**Fig. 13** Friction coefficients and wear mass loss of NiCrBSi−0.5$Y_2O_3$ composite coating vs load

The worn surface of the NiCrBSi−0.5$Y_2O_3$ composite coating under the load of 6 N is shown in Fig. 14 with its EDAX spectrum. It can be observed that some slight micro-cutting grooves develop on the worn

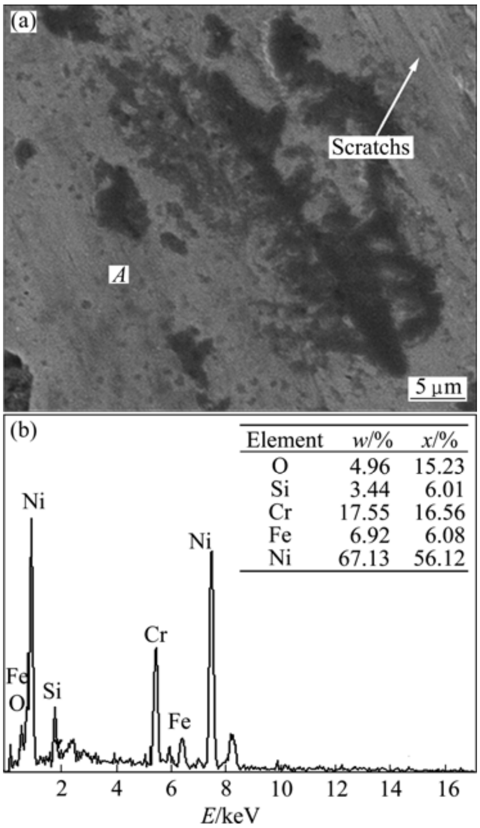

| Element | w/% | x/% |
|---|---|---|
| O | 4.96 | 15.23 |
| Si | 3.44 | 6.01 |
| Cr | 17.55 | 16.56 |
| Fe | 6.92 | 6.08 |
| Ni | 67.13 | 56.12 |

**Fig. 14** SEM image showing worn surface morphology (a) and EDAX spectrum (b) of NiCrBSi−0.5$Y_2O_3$ composite coating under load of 6 N

surface accompanied with a little oxide (Fig. 14(a)). The plough action of the wear debris is slight at low load due to the small depth of indention of the wear debris. The worn surface is composed of 4.96O, 3.44Si, 17.55Cr, 6.92Fe and 67.13Ni (Fig. 14(b)). It can be found that element O is much less under load of 6 N than at the load of 10 N (9.17%), which indicates less oxide at low load than at high load. This is because the friction oxidation reaction caused by friction heat is reduced at a low load. The wear mechanisms of the NiCrBSi−$Y_2O_3$ composite coating at a low load are adhesive wear and slight micro-cutting wear.

Figure 15 shows the worn surface and EDAX spectrum of the NiCrBSi−0.5$Y_2O_3$ composite coating at high load of 12 N. The worn surface is covered by the oxide film with the chemical composition of 1.51C, 11.23O, 3.70Si, 16.94Cr, 6.89Fe and 59.73Ni. The worn surface is severely oxidized with O content of 11.23% due to the severe friction heat in the shear process as a result of high contact stress at high loads. In addition, many plough grooves can be found in Fig. 15(a), indicating severe micro-cutting wear of the composite coating at high loads. It shows that the main wear mechanisms of the NiCrBSi−0.5$Y_2O_3$ composite coatings at high loads are adhesive wear and severe micro-cutting wear.

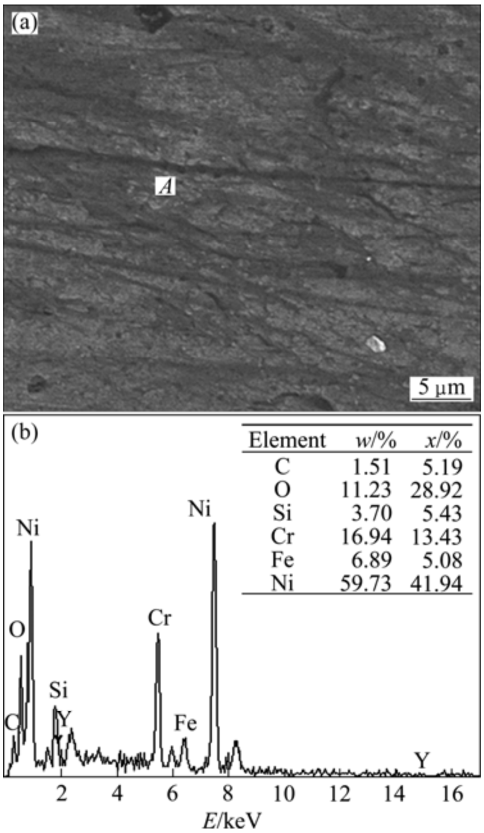

**Fig. 15** SEM image showing worn surface morphology (a) and EDAX spectrum (b) of NiCrBSi−0.5$Y_2O_3$ composite coating under load of 12 N

## 4 Conclusions

1) The plasma sprayed NiCrBSi−$Y_2O_3$ composite coatings are mainly composed of $\gamma$-Ni, CrB, $Cr_7C_3$ and $Y_2O_3$. With addition of $Y_2O_3$, hard phases such as CrB, $Cr_7C_3$ emerge in the composite coating, the density of the composite coatings also increases. The porosity of the NiCrBSi−$Y_2O_3$ composite coatings is less than 1%, much less than that of the pure NiCrBSi coating. The microhardness of the NiCrBSi−0.5$Y_2O_3$ composite coatings is about 1.2 times that of the pure NiCrBSi coating.

2) The NiCrBSi−0.5$Y_2O_3$ composite coating presents excellent tribological properties, whose friction coefficient is 0.175, 37% of the pure NiCrBSi coating. The wear mass loss of the composite coating is 1.2 mg, which is reduced by 43% compared with the pure NiCrBSi coating. The decreased friction coefficient of the composite coating can be attributed to the solid lubrication effect of the oxide film on the worn surface. At the loads of 6−10 N, the composite coating suffers from slight wear and the wear mechanisms are mainly adhesive wear accompany with slight micro-cutting wear and micro-fracture wear. As the load increases to 12 N, the wear of the composite coating becomes severe and the wear mechanisms are adhesive wear and severe micro-cutting wear.

## References

[1] GONZÁLEZ R, GARCÍA M A, PEÑUELAS I, CADENAS M, ROCÍO F M, HERNÁNDEZ B A, FELGUEROSO D. Microstructural study of NiCrBSi coatings obtained by different processes [J]. Wear, 2007, 263(1−6): 619−624.

[2] LIU Sheng-lin, ZHENG Xue-ping, GENG Gang-qiang. Dry sliding wear behavior and corrosion resistance of NiCrBSi coating deposited by activated combustion-high velocity air fuel spray process [J]. Materials and Design, 2010, 31(2): 913−917.

[3] PAN Jiao-liang, WANG Yin-zhen, LI Fang-po, GAO Hai-jun. Effect of $MoS_2$ coated with nickel on tribological properties of Ni-based coating [J]. Tribology, 2008, 28(3): 225−229. (in Chinese)

[4] CAI Bin, TAN Ye-fa, TU Yi-qiang, WANG Xiao-long, XU Ting. Effects of graphite content on microstructure and tribological properties of graphite/TiC/Ni-base alloy composite coatings [J]. Transactions of Nonferrous Metals Society of China, 2011, 21(8): 1741−1749.

[5] WANG Xin-hong, ZHANG Min, ZOU Zeng-da, QU Shi-yao. Microstructure and properties of laser clad TiCp/Ni-based alloys composite coating [J]. Chinese Journal of Mechanical Engineering, 2003, 39(2): 37−41. (in Chinese)

[6] ZHANG Shi-hong, LI Ming-xi, YOON J H, CHU T Y. Characterization on the coatings of Ni-base alloy with nano- and micron-size $Sm_2O_3$ addition prepared by laser deposition [J]. Materials Chemistry and Physics, 2008, 112(2): 668−674.

[7] WANG Hong-yu, XU Xiao-jing, CHEN Kang-min, ZHANG Xue-feng, LIU Xi. Effect of $La_2O_3$ on microstructure and properties

of Ni-based spray-welding coating on titanium alloys substrate [J]. Journal of the Chinese Rare Earth Society, 2005, 23(3): 339−344. (in Chinese)

[8] LI An-min, XU Bo-fan, PAN Ying-jun. Effects of $La_2O_3$ on microstructure and property of TiC/Ni-based composite coating [J]. Journal of Iron and Steel Research, 2003, 15(1): 57−61. (in Chinese)

[9] SHARMA S P, DWIVEDI D K, JAIN P K. Effect of $La_2O_3$ addition on the microstructure, hardness and abrasive wear behavior of flame sprayed Ni based coatings [J]. Wear, 2009, 267(2): 853−859.

[10] LI Jian-liang, XIONG Dang-sheng, HUANG Zhong-jia, KONG Jian, DAI Ji-hui. Effect of Ag and $CeO_2$ on friction and wear properties of Ni-base composite at high temperature [J]. Wear, 2008, 267(1): 576−584.

[11] ZHANG Zhen-yu, WANG Zhi-ping, LIANG Bu-nü. Microstructure and dry-sliding wear behavior of thermal sprayed and fused Ni-based coatings with the addition of $La_2O_3$ [J]. Tribology Letters, 2010, 37(2): 141−148.

[12] HAN Bao-lei, LU Xin-chun. Tribological and anti-corrosion properties of Ni−W−$CeO_2$ coatings against molten glass [J]. Surface & Coatings Technology, 2008, 202(14): 3251−3256.

[13] HUANG Jin-liang, TIAN Bao-hong, CHANG Lian-zhi. Effect of rare earth $CeO_2$ on the microstructure and tribological properties of laser remelted NiCrBSi-WC alloy coating [J]. Hot Working Technology, 1999(4): 3−6. (in Chinese)

[14] DAI Da-huang, ZHOU Ke-song, YUAN Zhen-hai. Surface technology science of modern materials [M]. Beijing: Metallurgical Industry Press, 2004. (in Chinese)

[15] KANG Rui-quan, LIU Wen-jin, MA Ming-xing, ZHONG Min-lin, ZHANG Wei-ming, ZHANG Hong-jun. The Effect of rare earth oxides oil particles distribution in laser cladding particles reinforced Ni-base composite coatings [J]. Applied Laser, 2009, 29(5): 374−378. (in Chinese)

[16] YANG Qing-xiang, ZHAO Yan-hui, LI Yan-li, YAO Mei. Thermodynamics of modifying effect of rare earth oxide on inclusions in hardfacing metal of medium-high carbon steel [J]. Journal of Rare Metals, 2002, 20(4): 291−294.

[17] LIU Guang-hua. Rare earth materials and their application technology [M]. Beijing: Chemistry Industry Press, 2005. (in Chinese)

[18] PAN Xiao-lin, SUN Wen-ru, YANG Shlin, GUO Shou-ren, LI Zhan, YANG Hong-cai, HU Zhuang-qi. Solidification and segregation behavior of GH742y alloy [J]. The Chinese Journal of Nonferrous Metals, 2008, 18(12): 2158−2165. (in Chinese)

[19] ZHOU Yong-jun, ZHANG Guo-ying. Study on electronic theory of the interaction between rare earth elements and impurities at grain boundaries in Ni-base superalloy [J]. Rare Metal Materials and Engineering, 2007, 36(12): 2160−2162. (in Chinese)

[20] WU Jian-jun, CAO Xiao-ming, WEN Ming. Modern technology of metallic thermal spray [M]. Beijing: Chemistry Industry Press, 2007. (in Chinese)

[21] LIU Xiu-bo, YU Rong-li. Effects of $La_2O_3$ on microstructure and wear properties of laser clad $\gamma$/$Cr_7C_3$/TiC composite coatings on TiAl intermatallic alloy [J]. Materials Chemistry and Physics, 2007, 101 (2−3): 448−454.

# NiCrBSi−$Y_2O_3$复合涂层的摩擦学行为与机理

蔡 滨，谭业发，谭 华，敬奇锋，张中威

解放军理工大学 野战工程学院，南京 210007

**摘 要：**运用等离子喷涂技术在45钢表面制备了NiCrBSi−$Y_2O_3$复合涂层，研究了其微观组织和摩擦学性能。结果表明：等离子喷涂NiCrBSi−$Y_2O_3$复合涂层主要由$\gamma$-Ni、CrB、$Cr_7C_3$和$Y_2O_3$等物相组成。在复合涂层中添加适量的$Y_2O_3$可增加CrB和$Cr_7C_3$等硬质相的含量，并提高复合涂层的致密度。当$Y_2O_3$含量(质量分数)为0.5%时，NiCrBSi−$Y_2O_3$复合涂层具有优异的摩擦学性能，其摩擦因数为0.175，仅为纯NiCrBSi涂层的37%；其磨损质量为1.2 mg，比纯NiCrBSi涂层的降低了43%。当载荷为6~10 N时，NiCrBSi−$Y_2O_3$复合涂层呈轻微磨损，其磨损机理主要为粘着磨损，并伴有轻微的微观切削和微观断裂磨损；当载荷达到12 N时，复合涂层产生严重磨损，其磨损机制转变为粘着磨损和严重的微观切削磨损。

**关键词：**等离子喷涂；复合涂层；NiCrBSi；$Y_2O_3$；摩擦；磨损

**(Edited by Hua YANG)**